Structure and Stability of Sulfur Trioxide−Ammonia Clusters with Water: Implications on Atmospheric Nucleation and Condensation

Peter M. Pawlowski, Steven R. Okimoto, and Fu-Ming Tao*

Department of Chemistry and Biochemistry, California State University, Fullerton, California 92834

Received: March 2, 2003; In Final Form: May 4, 2003

The structure and stability of the molecular clusters $NH_3 \cdot SO_3 \cdots (H_2O)_n$, $n = 1-6$, 9, 12, are studied using density functional theory. The results show that the electron donor/acceptor complex $NH_3 \cdot SO_3$ is stable with water and has an unusually high affinity for incoming water molecules. The complex itself is progressively stabilized by the addition of water molecules, as indicated by the shortening of the N−S bond distance with an increasing number of water molecules. The binding energy of the cluster to each H_2O molecule is about 12 kcal mol^{-1}, two to three times the binding energy of a pure water dimer, and it remains approximately constant as the cluster increases in size with an increasing number of H_2O molecules. The N−S distance decreases monotonically with the addition of each H_2O molecule, indicating that the $NH_3 \cdot SO_3$ unit in the clusters is stabilized by the introduced H_2O. The calculated group charge on SO_3 (or NH_3) increases as the N−S distance successively decreases, which reveals that the stability of the clusters originates from mutually enhanced electrostatic interactions between $NH_3 \cdot SO_3$ and H_2O. This study strongly suggests that $NH_3 \cdot SO_3$ may act as an effective nucleation agent for the formation of atmospheric aerosols and cloud particles.

Introduction

Nucleation is a vital process involved in phase transformations in laboratories and natural environments. Whether it be condensation, crystallization, or freezing, the conversion of one phase to another does not occur as spontaneously as predicted by simple thermodynamics-based bulk properties. Small clusters of molecules in a metastable phase are thermodynamically far different from the bulk system, and tend to dissipate due primarily to the entropy effect. As a result, homogeneous nucleation is typically an incredibly slow process. For example, at a relative humidity of 200% at 20 °C, water droplets nucleate at a mere 10^{-54} droplets per cm^3 per second. At such a rate, it would take $\sim 3.2 \times 10^{46}$ years for a single droplet to appear in a cubic centimeter of air.[1] However, rain droplets form in our atmosphere at relative humidities well below 200%. The solution to this apparent dilemma lies in the presence of preexisting particles, called cloud condensation nuclei (CCN), onto which water vapor precipitates at a much greater rate than onto itself. The production of CCN under homogeneous conditions usually relies on the presence of effective nucleation agents, chemical species of low vapor pressure and large affinity to the vapor molecules.

Sulfuric acid (H_2SO_4) is widely recognized as one of the most important such nucleation agents in the atmosphere; it is involved in both acid deposition and cloud formation.[2] In the gas phase, over 95% of the H_2SO_4 molecules exist as the binary complex $H_2SO_4 \cdots H_2O$ and larger clusters of hydrated H_2SO_4. The system has a significant binding energy with water, much greater than that of a pure water cluster, which leads to large equilibrium constants for the successive addition of a water molecule to the hydrated H_2SO_4. Thus, clusters of water form readily around H_2SO_4 or hydrated H_2SO_4, surpassing the critical size for nucleation. Extremely small amounts of H_2SO_4 are able to nucleate subsaturated H_2O vapor.[1]

Sulfuric acid can form by the reaction of sulfur trioxide (SO_3) with water in the atmosphere. The former is produced from the oxidation of sulfur dioxide (SO_2), which in turn originates either from anthropogenic and natural sources or from the oxidation of dimethyl sulfide (DMS).[2] However, the expected bimolecular formation reaction

$$SO_3 + H_2O \rightarrow H_2SO_4 \quad (1)$$

has been shown to have a high energy barrier of approximately 30 kcal mol^{-1}, and thus it cannot be the dominant pathway for sulfuric acid formation in the atmosphere. The energy barrier decreases when multiple water molecules are present,[3,4] as in the following pathway involving two water molecules:

$$SO_3 + H_2O \rightarrow H_2O \cdot SO_3 \quad (2)$$

$$H_2O \cdot SO_3 + H_2O \rightarrow H_2SO_4 \cdots H_2O \quad (3)$$

The energy barrier disappears completely in the presence of four or more water molecules.[4] This presents a major fate of atmospheric SO_3, which is well studied in the literature. Does sulfuric acid or hydrated H_2SO_4 represent the only major product of SO_3 in the natural atmosphere? Are there other effective nucleation reagents that originate from SO_3 and may play a significant role in the formation of atmospheric aerosols and cloud particles?

Ammonia (NH_3) is a significant atmospheric pollutant that may strongly interact with SO_3. Atmospheric NH_3 results from animal wastes, fertilizers, and automobile and industrial emissions. Leopold and co-workers[5] suggested that atmospheric SO_3 can associate with ammonia to form a zwitterionic sulfamic acid ($^+NH_3 \cdot SO_3^-$) via the following barrier-less reaction:

$$SO_3 + NH_3 \rightarrow NH_3 \cdot SO_3 \quad (4)$$

The complex has a much greater binding energy (∼20 kcal

* Corresponding author.

10.1021/jp034531w CCC: $25.00
Published on Web 06/13/2003

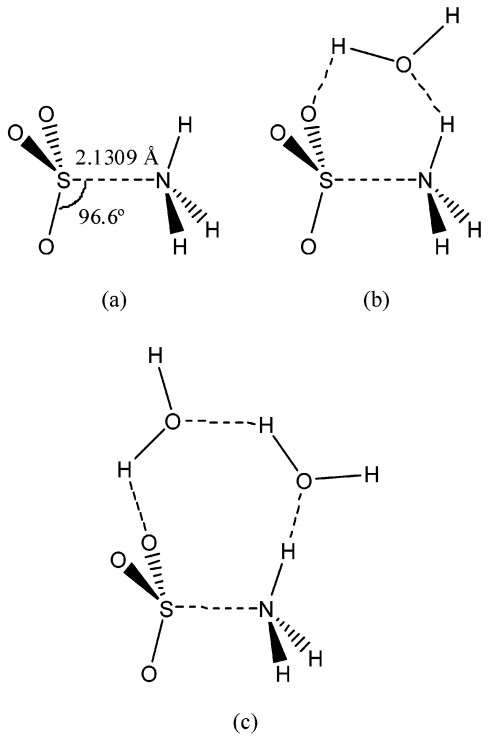

Figure 1. (a) Equilibrium geometry of the $NH_3 \cdot SO_3$ complex as calculated with the 6-311++G(d,p) basis set. (b) Favorable hydrogen-bonding of a single H_2O to a site of the complex or (c) of two H_2O molecules to a single site of the complex.

mol^{-1})[6,7] than the association of SO_3 with H_2O to form $H_2O \cdot SO_3$ (7.9 kcal mol^{-1}).[8] An orbital overlap between NH_3 and SO_3 results in the shift of electron density of the nitrogen toward the sulfur in an electron donor−acceptor (EDA) interaction between SO_3 and NH_3. Previous computational studies[9,10] have shown that the equilibrium geometry of the $NH_3 \cdot SO_3$ complex is staggered, as given in Figure 1a.

According to the recent theoretical work,[10] the $NH_3 \cdot SO_3$ complex remains intact when attacked by an H_2O molecule. The transformation of $NH_3 \cdot SO_3 \cdots H_2O$, a complex of $NH_3 \cdot SO_3$ hydrogen-bonded with a H_2O molecule, to $H_2O \cdot SO_3 \cdots NH_3$ is endothermic with a high barrier of approximately 21.4 kcal mol^{-1}. The increased stability of the $NH_3 \cdot SO_3$ complex in the presence of additional H_2O molecules would strongly suggest that this complex could act as a nucleation agent without turning SO_3 into H_2SO_4 or other sulfate products.

Atmospheric H_2O concentrations are typically much higher than those of NH_3 (tropospheric boundary layer mixing ratios of $\sim 10^{-2}$ versus 10^{-11} to 10^{-9}).[6] Under certain conditions, however, the reaction of SO_3 and NH_3 may play a significant role. The rate constant for the formation of the $NH_3 \cdot SO_3$ complex is more than 4 orders of magnitude greater than that of H_2SO_4.[11] Moreover, as mentioned earlier, $NH_3 \cdot SO_3$ has a higher binding energy than $H_2O \cdot SO_3$ or $H_2SO_4 \cdots H_2O$ (20 kcal mol^{-1} versus about 8 kcal mol^{-1}).[6−9] The likely role of NH_3 in atmospheric nucleation was observed by Weber et al.[12] His group found in field studies at the Mauna Loa Observatory in Hawaii that atmospheric nucleation rates were significantly higher than expected from a pure $H_2SO_4 \cdots H_2O$ system, and they suggest ammonia could play a role in this increase. In another study, the same group detected unusually high concentrations of the smallest measurable ultra-fine particles downwind from a penguin colony, a considerable source of NH_3.[13] Both these results suggest that SO_3 and NH_3 may be important in atmospheric nucleation.

The present study systematically investigates the structure and stability of water clusters containing a unit of $NH_3 \cdot SO_3$ in an attempt to evaluate the role of the $NH_3 \cdot SO_3$ complex in atmospheric nucleation. Quantum mechanical calculations of the clusters are carried out using density functional theory. The successive binding energies and other related molecular properties of the $NH_3 \cdot SO_3 \cdots (H_2O)_n$ clusters are analyzed and compared to those of pure water clusters. Our primary goal is to show that the $NH_3 \cdot SO_3$ complex is highly stable in water clusters with a consistently strong affinity for incoming water molecules and that it may therefore play an important role in atmospheric nucleation.

Theoretical Background

The molecular clusters considered in this study, $NH_3 \cdot SO_3 \cdots (H_2O)_n$, were formed by the successive addition of H_2O molecules to the $NH_3 \cdot SO_3$ complex. The largest cluster contains twelve H_2O molecules surrounding the $NH_3 \cdot SO_3$ unit. Each H_2O molecule was introduced for maximum stability based on favorable electrostatic and hydrogen bonding interactions. As a result, only the most stable geometries were carefully examined and reported, although other likely candidates were also attempted.

The equilibrium geometry for the $NH_3 \cdot SO_3$ complex exhibits C_3 symmetry (see Figure 1a). Three discrete sites for H_2O placement are designated and the numbers of H_2O at the site are n_1, n_2, and n_3, respectively. For the first six H_2O molecules, up to two connecting waters were placed at each site, with appropriate hydrogen bonding (see Figure 1b,c). Complexes with three or more connecting water molecules at each site were attempted, but these configurations were not pursued because the resulting clusters were significantly less stable. In the clusters with 9 or 12 H_2O molecules, two connecting waters were placed directly at each site, and the rest were distributed between the sites. All clusters considered are designated $NH_3 \cdot SO_3 \cdots (H_2O)_n$ (n_1,n_2,n_3), or n(n_1,n_2,n_3) in short, where n_i is the number of H_2O molecules at site i. For consistency, the complexes with nine and twelve water molecules are still referred to as $NH_3 \cdot SO_3 \cdots (H_2O)_9$ (3,3,3) and $NH_3 \cdot SO_3 \cdots (H_2O)_{12}$-(4,4,4), respectively, or 9(3,3,3), 12(4,4,4) in short, although only two connecting H_2O molecules are present at each site and the remainder are disturbed as described above. Many redundant configurations exist as a result of symmetry, and therefore n_1 is incremented before n_2, and likewise, n_2 before n_3. The C_3 symmetry was imposed in the search for the following clusters: 3(1,1,1), 6(2,2,2), 9(3,3,3), and 12(4,4,4).

The initial geometries described above were optimized using density functional theory (DFT). The DFT method employed was Becke's three-parameter functional method[14−16] with the nonlocal correlation of Lee, Yang, and Parr (B3LYP).[17] Previous studies establish this technique as reliable for stable closed-shell molecules and hydrogen-bonded complexes such as those considered in this study.[18] Each cluster was calculated with two relatively large basis sets, 6-31+G(d) and 6-311++G(d, p). The diffuse functions in these basis sets are required for accurate computation of delocalized interactions such as the hydrogen bonding and EDA interactions in this study. The results obtained from the two basis sets are similar and thus only the data from the larger basis set is reported.

Total intermolecular energies of the clusters, ΔE_T, were determined relative to $NH_3 \cdot SO_3$ and the separate H_2O molecules. Such energies may also be recognized as the total binding energies (D_e) of $NH_3 \cdot SO_3$ for all H_2O molecules within the clusters. Note that there is a sign change, i.e., $D_e = -\Delta E_T$. The

TABLE 1: Equilibrium Bond Lengths (in Å), Bond Angles (°), and Total Energies (H) of the Monomers and the $NH_3 \cdot SO_3$ Complex Calculated Using the B3LYP Method with the 6-311++G(d,p) Basis Set

	parameter	experimental[a]	6-311++G(d,p)
H_2O			
	r(OH)	0.9575	0.9620
	∠(HOH)	104.51	105.06
	E		−76.458531
NH_3			
	r(NH)	1.012	1.0144
	∠(HNH)	106.7	107.9
	E		−56.582722
SO_3			
	r(SO)	1.4198	1.4467
	E		−623.856479
$NH_3 \cdot SO_3$			
	r(NS)	1.957	2.1309
	∠(NSO)	97.6	96.6

[a] Experimental values for H_2O, NH_3, and SO_3 are from ref 23, while experimental values for $NH_3 \cdot SO_3$ are from ref 6.

TABLE 2: Bond Length *r*(NS) (Å), Total Energy *E* (Hartree), Total H_2O Binding Energies ΔE_T (kcal mol^{-1}), and Binding Energies per H_2O, $\Delta E/H_2O$, (kcal mol^{-1}) Calculated for the $NH_3 \cdot SO_3 \cdots (H_2O)_n$ clusters using the B3LYP method with the 6-311++G(d,p) Basis Set

				6-311++G(d,p)			
n	n_1	n_2	n_3	*r*(NS)	*E*	ΔE_T	$\Delta E/H_2O$
0	0	0	0	2.1309	−680.471467		
1	1	0	0	2.0283	−756.948744	−11.8	−11.8
2	1	1	0	1.9564	−833.426095	−23.6	−11.8
2	2	0	0	1.9772	−833.427045	−24.2	−12.1
3	1	1	1	1.9097	−909.903003	−35.1	−11.7
3	2	1	0	1.9251	−909.904245	−35.9	−12.0
4	2	1	1	1.8827	−986.380828	−47.2	−11.8
4	2	2	0	1.8888	−986.382391	−48.2	−12.0
5	2	2	1	1.8551	−1062.858345	−59.1	−11.8
6	2	2	2	1.8333	−1139.336302	−71.3	−11.9
9	3	3	3	1.7939	−1368.761456	−102.4	−11.4
12	4	4	4	1.7884	−1598.188697	−134.8	−11.2

successive binding energy was calculated by averaging the total binding energy over the number of H_2O molecules present in the given cluster. All DFT calculations were performed using the GAUSSIAN 98 computational chemistry package.[19] The molecular graphics were created using the Molekel Molecular Visualizations Package.[20,21]

Results and Discussion

The equilibrium geometries of the NH_3, SO_3, and H_2O monomers and the $NH_3 \cdot SO_3$ complex were optimized and the relevant parameters are presented in Table 1. The calculated geometrical values are in agreement with experimental data. For example, the calculated N−S distance and N−S−O angle of the $NH_3 \cdot SO_3$ complex, 2.131 Å and 96.6°, respectively, are comparable to 1.957 Å and 97.6° obtained by Canagaratna et al.[6] from a microwave spectroscopy study.

Table 2 presents the calculated N−S distances, total electronic energies, binding energies for all H_2O molecules, and successive binding energies for the $NH_3 \cdot SO_3 \cdots (H_2O)_n$ clusters. Table 3 shows whole-molecule partial charges for NH_3 and SO_3 from Mullikan population analysis, along with the three N−S−O angles designated θ_1, θ_2, and θ_3. Figure 2 depicts the equilibrium geometries calculated for all $NH_3 \cdot SO_3 \cdots (H_2O)_n$ clusters considered. The dotted gray lines in the figure represent hydrogen bonds.

In all $NH_3 \cdot SO_3 \cdots (H_2O)_n$ clusters, each H_2O molecule participates in double hydrogen bonding, acting as both acceptor and donor. In the case of the $n = 1$ cluster, as shown in Figure 1b, where a single H_2O is present, the H_2O donates a hydrogen bond to an oxygen atom of SO_3 while accepting a hydrogen bond from a hydrogen atom of NH_3. In the cluster 2(2,0,0), as shown in Figure 1c, the two H_2O molecules are connected via a hydrogen bond; one of them donates a hydrogen bond to SO_3 while the other accepts one from the NH_3.

TABLE 3: The Group Charges, $\delta^-(SO_3)$ and $\delta^+(NH_3)$, and the N−S−O Bond Angles, θ_1, θ_2, and θ_3 (°), Calculated for the $NH_3 \cdot SO_3 \cdots (H_2O)_n$ Clusters Using the B3LYP Method with the 6-311++G(d,p) Basis Set

				6-311++G(d,p)				
n	n_1	n_2	n_3	$\delta^-(SO_3)$	$\delta^+(NH_3)$	θ_1	θ_2	θ_3
0	0	0	0	−0.275	0.275	96.6	96.6	96.6
1	1	0	0	−0.368	0.356	98.0	97.4	99.1
2	1	1	0	−0.449	0.414	99.6	98.9	100.2
2	2	0	0	−0.401	0.394	98.7	99.1	99.1
3	1	1	1	−0.506	0.453	100.7	100.6	100.7
3	2	1	0	−0.480	0.448	100.0	99.5	100.7
4	2	1	1	−0.539	0.485	101.1	100.7	101.6
4	2	2	0	−0.503	0.481	100.7	100.4	101.1
5	2	2	1	−0.576	0.531	101.7	102.1	101.2
6	2	2	2	−0.597	0.525	102.2	102.2	102.2
9	3	3	3	−0.708	0.547	103.5	103.5	103.5
12	4	4	4	−0.773	0.666	103.6	103.6	103.6

The addition of H_2O molecules to $NH_3 \cdot SO_3$ apparently increases the stability of the $NH_3 \cdot SO_3$ unit within the clusters. The solid plot in Figure 3 shows the N−S distance as a function of *n*, the total number of H_2O molecules. It is clear from this plot that the addition of each H_2O molecule shortens the N−S distance in every case considered. A shorter N−S distance corresponds to a larger EDA interaction in the $NH_3 \cdot SO_3$ unit and thus a more stable $NH_3 \cdot SO_3$ unit. For a given *n*, the cluster with more evenly distributed H_2O molecules exhibited a shorter N−S distance. For example, 2(1,1,0) exhibits a shorter N−S distance than 2(2,0,0). The shorter N−S distance was used in Figure 3 whenever two possible configurations were obtained for the cluster of a given *n* ($n = 2-4$).

It is plausible to argue that the shortening N−S distance results from an H_2O-facilitated mechanical-pulling effect. In other words, the hydrogen bonds established by H_2O pull between the oxygen atom of SO_3 and the hydrogen atom of NH_3 and bring the two closer, causing the decrease of the N−S distance. However, the partial charge data may provide a more convincing explanation. As shown by the broken plot in Figure 3, the partial charge δ^- on the entire SO_3 molecule generally becomes more negative as the number of H_2O molecules increases. The similarity between the two lines in Figure 3 is unmistakable, and one can conclude that the partial charge is well correlated with the N−S bond distance. The most likely explanation for this phenomenon lies in the polar nature of water. The H_2O molecules are oriented to favor the charge/electrostatic interactions with charged NH_3 and SO_3, further enhancing the charge separations between the two subunits. This, in turn, strengthens the $NH_3 \cdot SO_3$ EDA interaction by shortening the N−S distance, yielding a more stable entity of $NH_3 \cdot SO_3$. The role of H_2O in stabilizing $NH_3 \cdot SO_3$ is thus straightforward.

It is interesting to examine the interaction energies or binding energies of the clusters toward each incoming H_2O molecule. As shown in Table 2, such energies, ranging from −11.2 to −12.1 kcal mol^{-1}, are large and approximately constant with the growth of the clusters. This implies that the $NH_3 \cdot SO_3$ complex has a large affinity for H_2O from the start and this affinity does not diminish as the cluster grows. This feature is in high

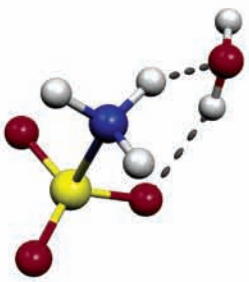

(a) $NH_3 \bullet SO_3 \cdots (H_2O)_1$ (1,0,0)

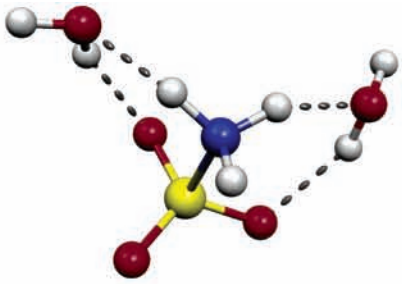

(b) $NH_3 \bullet SO_3 \cdots (H_2O)_2$ (1,1,0)

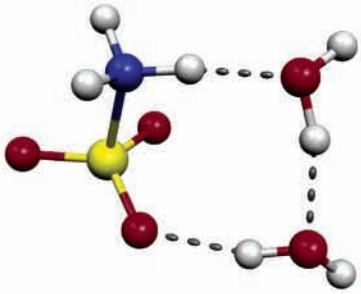

(c) $NH_3 \bullet SO_3 \cdots (H_2O)_2$ (2,0,0)

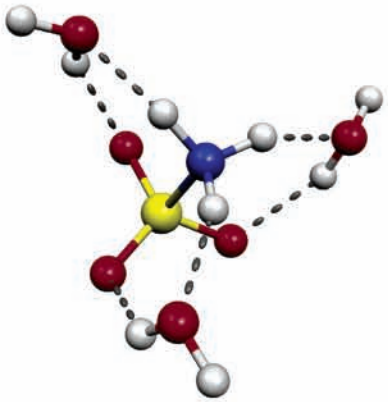

(d) $NH_3 \bullet SO_3 \cdots (H_2O)_3$ (1,1,1)

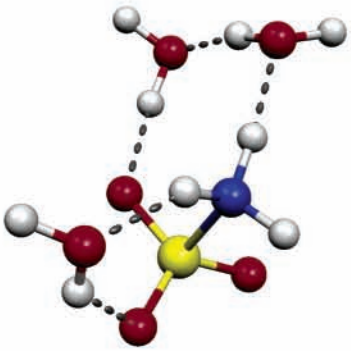

(e) $NH_3 \bullet SO_3 \cdots (H_2O)_3$ (2,1,0)

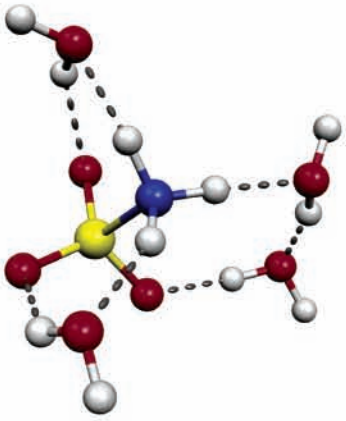

(f) $NH_3 \bullet SO_3 \cdots (H_2O)_4$ (2,1,1)

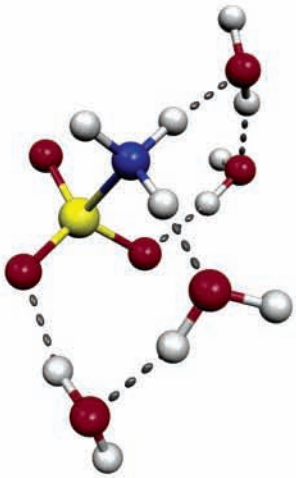

(g) $NH_3 \bullet SO_3 \cdots (H_2O)_4$ (2,2,0)

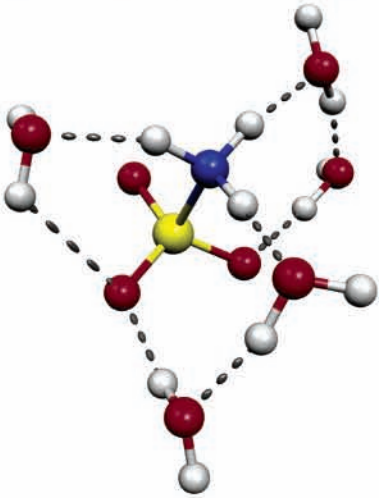

(h) $NH_3 \bullet SO_3 \cdots (H_2O)_5$ (2,2,1)

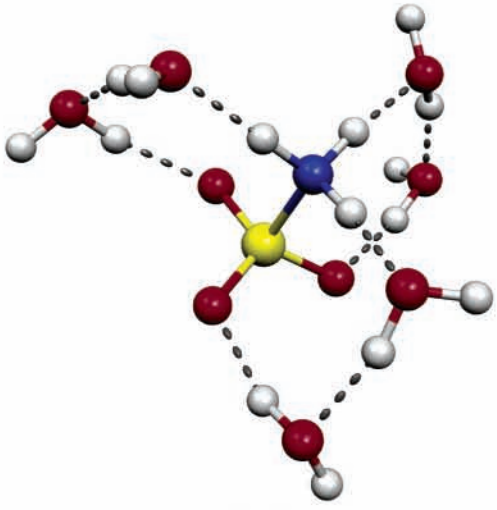

(i) $NH_3 \bullet SO_3 \cdots (H_2O)_6$ (2,2,2)

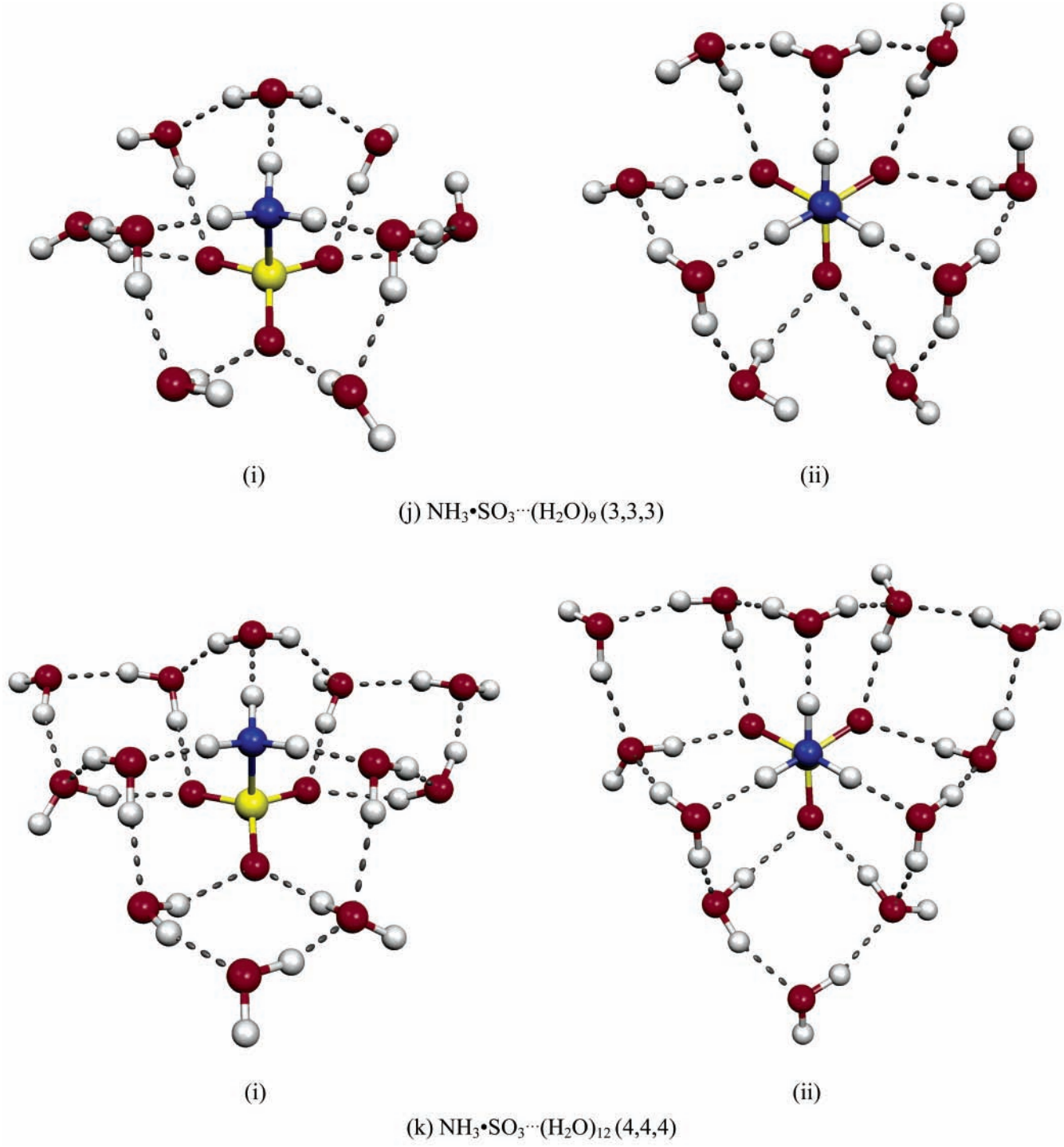

Figure 2. Equilibrium geometries for all $NH_3 \cdot SO_3 \cdots (H_2O)_n$ clusters considered.

contrast with that of pure water clusters. Figure 4 compares the successive H_2O binding energies of $NH_3 \cdot SO_3 \cdots (H_2O)_n$ with those of the pure water clusters $H_2O \cdots (H_2O)_n$. The binding energy of the first H_2O to the $NH_3 \cdot SO_3$ is 11.8 kcal mol^{-1} compared to the binding energy of only 4.9 kcal mol^{-1} for $(H_2O)_2$.[22] With the exception of the case of $n = 3$, all successive binding energies of $(H_2O)_n$ are lower than that of $NH_3 \cdot SO_3 \cdots (H_2O)_n$. The $(H_2O)_4$ cluster appears exceptionally stable, which leads to an unusually large binding energy for $n = 3$, because the H_2O molecules form a cyclic structure where each water acts as both a hydrogen bond acceptor and a donor at the favorable orientation. The consistently higher binding energies of $NH_3 \cdot SO_3 \cdots (H_2O)_n$ mean a greater potential for such clusters to attract and maintain H_2O molecules than the corresponding pure water clusters.

Implications

The immediate implication of the results is that the $NH_3 \cdot SO_3$ complex may act as a potent natural agent for initiating homogeneous nucleation processes in water vapor and other atmospheric environments. The complex may play an important role in large-scale atmospheric phenomena such as the formation of aerosols and cloud particles. Sulfuric acid, sulfate, and various other salt components have long been identified as primary agents for atmospheric nucleation. The findings of this study suggest that $NH_3 \cdot SO_3$ should be added to this list of such agents

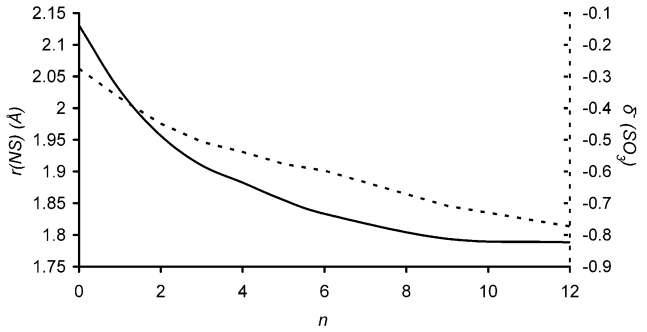

Figure 3. Plot of the bond distance r(NS) of the $NH_3{\cdot}SO_3{\cdots}(H_2O)_n$ cluster as a function of n, the number of H_2O molecules in the cluster (solid line), as well as the plot of the group charge $\delta^-(SO_3)$ calculated for the $NH_3{\cdot}SO_3{\cdots}(H_2O)_n$ cluster as a function of n (broken line).

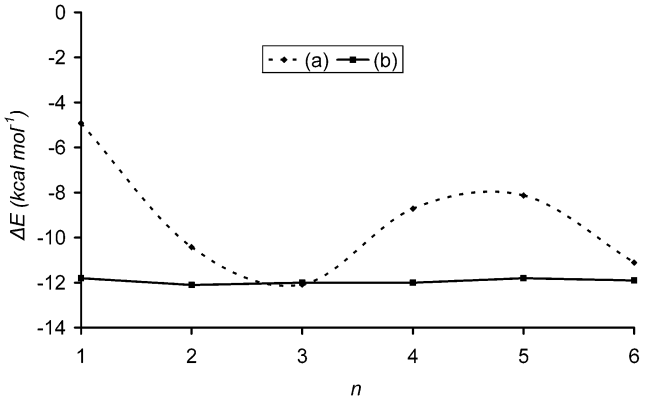

Figure 4. Comparison of the binding energy per H_2O molecule for (a) pure water clusters (ref 22), $(H_2O)_n$, and (b) $NH_3{\cdot}SO_3{\cdots}(H_2O)_n$.

responsible for atmospheric nucleation and subsequent natural phenomena.

The present work further confirms the conclusion of the previous study[10] that the $NH_3{\cdot}SO_3$ complex is a stable entity once it is formed. However, the question remains as to how significant is the actual concentration of $NH_3{\cdot}SO_3$ in the natural atmosphere. Atmospheric concentrations of H_2O are usually 7 to 9 orders of magnitude higher than those of NH_3.[6] Therefore, SO_3 would more likely encounter H_2O and eventually form H_2SO_4. This is the probable fate of SO_3 in the atmospheric conditions of high humidity and low concentrations of NH_3.

However, in heavily polluted atmospheres, the concentration ratio $[NH_3]/[H_2O]$ can be greater than 10^{-4}. In such cases, SO_3 might more likely join with NH_3, resulting in the stable $NH_3{\cdot}SO_3$ complex. The binding energy for $NH_3{\cdot}SO_3$, about 20 kcal mol^{-1}, is much larger than that for $H_2O{\cdot}SO_3$, about 8 kcal mol^{-1}. Accordingly, the equilibrium constant for $NH_3 + SO_3 \rightleftharpoons NH_3{\cdot}SO_3$ is several orders of magnitude larger than that for $H_2O + SO_3 \rightleftharpoons H_2O{\cdot}SO_3$. As a result, NH_3 is able to compete against H_2O to form the more stable $NH_3{\cdot}SO_3$ complex. The $H_2O{\cdot}SO_3$ complex has a smaller binding energy than the water−nitric acid complex ($H_2O{\cdot}HNO_3$). Less than 1% of HNO_3 was hydrated under all atmospheric conditions.[25] Consequently, less than 1% of the SO_3 in the natural atmosphere is expected to be the hydrated form of $H_2O{\cdot}SO_3$. Therefore, the majority of SO_3 exists in the monomeric form and is free to form the $NH_3{\cdot}SO_3$ complex.

The subsequent introduction of H_2O to $NH_3{\cdot}SO_3$ simply leads to larger clusters consisting of increasingly more stable $NH_3{\cdot}SO_3$ core units. As shown in this work, such clusters have consistently large binding energies for incoming H_2O molecules, which may suggest that the $NH_3{\cdot}SO_3$ complex is a potent agent for initiating homogeneous nucleation processes involving water vapor and that it plays an important role in the formation of cloud and aerosol particles in certain atmospheric conditions. Weber et al.[13] made a similar assertion about the role of NH_3, as supported by their detection of high concentrations of the smallest measurable ultra-fine particles downwind from a penguin colony, a considerable source of NH_3. However, they focused on the possibility of $NH_3-H_2SO_4$ and the corresponding salts, rather than $NH_3{\cdot}SO_3$.

It remains unclear about the eventual fate of the water clusters of $NH_3{\cdot}SO_3$ in the natural atmosphere. Various pathways for breaking the N−S bond in water clusters were examined but failed to identify any feasible channel with a low energy barrier for the dissociation of $NH_3{\cdot}SO_3$.[10,24] Lovejoy and Hanson[6] proposed that $NH_3{\cdot}SO_3$ might be scavenged by aerosols, but they did not provide any evidence or details. It would be interesting to know how NH_3 is released from $NH_3{\cdot}SO_3$ and SO_3 is converted into sulfate in a natural environment. The present study has ruled out the possibility of the dissociation of $NH_3{\cdot}SO_3$ in the water vapor or aqueous state. It indicates that such a process may require a heterogeneous condition involving other chemical species.

Conclusion

Molecular clusters consisting of the electron donor/acceptor complex $NH_3{\cdot}SO_3$ and up to 12 water molecules have been studied using density functional theory. The equilibrium geometries and energies were calculated for the stable clusters in which the water molecules interact with $NH_3{\cdot}SO_3$ via favorable electrostatics and hydrogen bonding. The results show that the $NH_3{\cdot}SO_3$ complex is stable in the water clusters and has an unusually high affinity for incoming water molecules. The complex is progressively stabilized by water molecules, as indicated by the shortening of the N−S bond distance with an increasing number of water molecules. The binding energy of the cluster with each additional H_2O molecule is about 12 kcal mol^{-1} and remains approximately constant as the cluster increases in size. The stability of the clusters can be understood on the basis of calculated partial charges on NH_3 and SO_3. The study strongly suggests that $NH_3{\cdot}SO_3$ may act as a very effective nucleation agent in the formation of atmospheric aerosols and cloud particles.

Acknowledgment. This work was supported in part by The Research Corporation (Award No. CC4121) and The Camille and Henry Dreyfus Foundation (Award No. TH-00-028). Fu-Ming Tao is a Henry Dreyfus Teacher/Scholar for 2001−2005. The authors also thank Professor Kenneth R. Leopold of the University of Minnesota for helpful discussions.

References and Notes

(1) Seinfeld, J. H.; Pandis, S., N. *Atmospheric Chemistry and Physics: From Air Pollution to Climate Change*; John Wiley and Sons: New York, 1998.

(2) Finalyson-Pitts, B. J.; Pitts, J. N., Jr. *Chemistry of the Upper and Lower Atmosphere*; Academic Press: San Diego, 2000.

(3) Morokuma, K.; Muguruma, C. *J. Am. Chem. Soc.* **1994**, *116*, 10316.

(4) Larson, L. J.; Kuno, M.; Tao, F.-M. *J. Chem. Phys.* **2000**, *112*, 8830.

(5) Canagaratna, M.; Phillips, J. A.; Goodfriend, H.; Leoplold, K. R. *J. Am. Chem. Soc.* **1996**, *118* (22), 5290.

(6) Lovejoy, E. R.; Hanson, D. R. *J. Phys. Chem.* **1996**, *100*, 4459.

(7) Wong, M. W.; Wilberg, K. B.; Frisch, M. K. *J. Am. Chem. Soc.* **1992**, *114*, 523.

(8) Hoffmann, M.; Schleyer, P. v. R. *J. Am. Chem. Soc.* **1994**, *116*, 4947.

(9) Hickling, S. J.; Woolley, R. G. *Chem. Phys. Lett.* **1990**, *116*, 43.

(10) Larson, L. J.; Tao, F.-M. *J. Phys. Chem. A* **2001**, *105*, 4344−4350.
(11) Shen, G.; Suto, M.; Lee, L. C. *J. Geophys. Res.* **1990**, *95*, 13981.
(12) Weber, R. J.; McMurry, P. H.; Eisle, F. L.; Tanner, D. J. *J. Atmos. Sci.* **1995**, *52*, 2242.
(13) Weber, R. J.; McMurry, P. H.; Mauldin, L.; Tanner, D. J.; Eisle, F. L.; Brechtel, F. J.; Kreidenweis, S. M.; Kok, G. L.; Schillawski, R. D.; Baumgardner, D. *J. Geophys. Res.* **1998**, *103*, 16385.
(14) Becke, A. D. *J. Chem. Phys.* **1992**, *96*, 2155.
(15) Becke, A. D. *J. Chem. Phys.* **1992**, *97*, 9193.
(16) Becke, A. D. *J. Chem. Phys.* **1993**, *98*, 5648.
(17) Lee, C.; Yang, W.; Parr, R. G. *Phys. Rev. B* **1988**, *37*, 785.
(18) Topol, I. A.; Burt, S. K.; Rashin, A. A. *Chem. Phys. Lett.* **1995**, *247*, 112.
(19) Frisch, M. J.; Trucks, G. W.; Schlegel, H. B.; Scuseria, G. E.; Robb, M. A.; Cheeseman, J. R.; Zakrzewski, V. G.; Montgomery, J. A., Jr.; Stratmann, R. E.; Burant, J. C.; Dapprich, S.; Millam, J. M.; Daniels, A. D.; Kudin, K. N.; Strain, M. C.; Farkas, O.; Tomasi, J.; Barone, V.; Cossi, M.; Cammi, R.; Mennucci, B.; Pomelli, C.; Adamo, C.; Clifford, S.; Ochterski, J.; Petersson, G. A.; Ayala, P. Y.; Cui, Q.; Morokuma, K.; Malick, D. K.; Rabuck, A. D.; Raghavachari, K.; Foresman, J. B.; Cioslowski, J.; Ortiz, J. V.; Baboul, A. G.; Stefanov, B. B.; Liu, G.; Liashenko, A.; Piskorz, P.; Komaromi, I.; Gomperts, R.; Martin, R. L.; Fox, D. J.; Keith, T.; Al-Laham, M. A.; Peng, C. Y.; Nanayakkara, A.; Gonzalez, C.; Challacombe, M.; Gill, P. M. W.; Johnson, B. G.; Chen, W.; Wong, M. W.; Andres, J. L.; Head-Gordon, M.; Replogle, E. S.; Pople, J. A. *Gaussian 98*, Revision A.9; Gaussian, Inc.: Pittsburgh, PA, 1998.
(20) Flükiger, P.; Lüthi, H. P.; Portmann, S.; Weber, J. *MOLEKEL 4.2*; Swiss Center for Scientific Computing: Manno, Switzerland, 2000−2002.
(21) Portmann, S.; Lüthi, H. P. *CHIMIA* **2000**, *54*, 766.
(22) Maheshwary, S.; Patel, N.; Sathyamurthy, N.; Kulkarni, A. D.; Gadre, S. R. *J. Phys. Chem. A* **2001**, *105*, 10525−10537.
(23) *CRC Handbook of Chemistry and Physics*, *80*th ed.; Lide, D. R., Ed.; CRC: Boca Raton, FL, 1999.
(24) Okimoto, S. R.; Tao, F.-M. Unpublished work.
(25) Tao, F.-M.; Higgins, K.; Klemperer, W.; Nelson, D. D. *Geophys. Res. Lett.* **1996**, *23*, 1797.